Peer-reviewed version available at *Materials* **2017**, *10*, 1394; doi:10.3390/ma10121394

Article

Grain refinement kinetics in a low alloyed Cu-Cr-Zr alloy subjected to large strain deformation

Anna Morozova [1,*], Elijah Borodin [2], Vladimir Bratov [2,3], Sergey Zherebtsov [1], Andrey Belyakov [1] and Rustam Kaybishev [1]

[1] Belgorod State University, Russia; morozova_ai@bsu.edu.ru, belyakov@bsu.edu.ru, zherebtsov@bsu.edu.ru, rustam_kaibyshev@bsu.edu.ru
[2] Institute of Problems of Mechanical Engineering RAS, Saint-Petersburg, Russia; elbor7@gmail.com
[3] Saint-Petersburg State University, Saint-Petersburg, Russia; vladimir.bratov@gmail.com
* Correspondence: morozova@bsu.edu.ru; Tel.: +7-904-083-9135

Abstract: The microstructure evolution and grain refinement kinetics of a solution treated Cu – 0.1Cr – 0.06Zr alloy during equal channel angular pressing (ECAP) at a temperature of 673 K via route B_C were investigated. The microstructure change during plastic deformation was accompanied by the microband formation and an increase in the misorienations of strain-induced subboundaries. The refinement of initial coarse grains was considered as a result of continuous dynamic recrystallization. The dynamic recrystallization kinetics was discussed in terms of grain/subgrain boundary triple junction evolution. The strain dependence of the triple junctions of high-angle boundaries can be expressed by a modified Johnson-Mehl-Avrami-Kolmogorov relationship with a strain exponent of about 1.49. Severe plastic deformation by ECAP led to substantial strengthening of the Cu-0.1Cr-0.06Zr alloy. The yield strength increased from 60 MPa in the initial state to 445 MPa after the total strain of 12.

Keywords: Cu-Cr-Zr alloy; grain refinement; severe plastic deformation; triple junctions; grain refinement kinetics

1. Introduction

The Cu-Cr-Zr alloys are one of typical Cu-base precipitation hardening type alloys, which were designed to exhibit both high electrical conductivity and high strength [1-11]. These alloys are advanced materials for railway contact wire, resistance welding electrodes, electronic commutators, etc. [2, 12]. There is a demand for high speed electric railways to increase the strength and electroconductivity of contact wires [4, 13]. The strength of Cu-Cr-Zr alloy can be significantly enhanced through grain refinement in accordance with the Hall – Petch equitation [14-21]. One of promising methods for grain refinement and hardening of various metallic materials including copper and Cu-Cr-Zr alloys is severe plastic deformation [15, 18-33]. Recently, many techniques of severe plastic deformation such as high pressure torsion [6, 22-23], multidirectional forging [24, 25], accumulative roll-bonding [26] and equal channel angular pressing [4, 18-21, 27-32], have been developed to obtain an ultra-fine grained structure in metals and alloys. Most of this specific technique is used only for laboratory simulations at present time. The main advantage of ECAP is the possibility of its industrial application as the ECAP-Conform to process large semi-products [21-23]. The ECAP-Conform-processing can be used in continuous line of rod or wire production [33-36]. The microstructures and mechanical properties developed after ECAP and ECAP-Conform have been confirmed being the same [33]. The necessary properties, such as strength and electroconductivity, can be obtained by controlling the development of the ultra-fine grained structure during large strain plastic deformation.

The development of ultra-fine grained structures in copper and its alloys during severe plastic deformation results from a type of a continuous dynamic recrystallization, in which the grain refinement can be considered as an evolution of the deformation substructures [19-21, 37-40]. During

Preprints (www.preprints.org) | NOT PEER-REVIEWED | Posted: 1 December 2017 doi:10.20944/preprints201712.0009.v1

Peer-reviewed version available at *Materials* **2017**, *10*, 1394; doi:10.3390/ma10121394

continuous dynamic recrystallization the strain-induced low-angle boundaries gradually transform into high-angle boundaries with an increase in the total strain. As a result, the ultra-fine grained structure with high dislocation density evolves at large strains [19-21, 37-41].

It is important in the dynamic recrystallization that new low-angle boundaries form and increase their misorientations during deformation. The continuous dynamic recrystallization development can be characterized by the mean angle of boundary misorientations, the fraction of low-angle and high-angle boundaries, the distribution of boundary misorientations and also the nature and distribution of boundary triple junctions formed by the new strain-induced (sub)boundaries. However, the triple junction analysis has not been reported in scientific literature. The model distribution of the triple junctions including special and ordinary grain boundaries has been briefly discussed [42]. In general, triple junctions in deformed materials can be formed by three low-angle boundaries (J0), one high-angle and two low-angle boundaries (J1), two high-angle and one low-angle boundary (J2) and three high-angle boundaries (J3). The developing microstructure should correspond to the specific triple junction distribution. Thus, at relativity small strains, large fraction of J0 and small fraction of J3 are expected. On the other hand, the J3 fraction in the dynamically recrystallized ultra-fine grained structure after large strain deformations should be approximately 1. Therefore, the study of the triple junction evolution can be used as a new approach to follow the microstructural changes and the kinetics of grain refinement process.

It has been shown in [43-45] that the progress in discontinuous dynamic recrystallization complies with normal Avrami kinetics, and the recrystallized fraction (F_{DRX}) can be related to a strain (ε) through a modified Johnson-Mehl-Avrami-Kolmogorov equation,

$$F_{DRX} = 1 - \exp(-k\,\varepsilon^{n}), \tag{1}$$

where k and n are constants, which depend on the material nature and processing conditions.

The development of the ultra-fine grained structure during cold-to-warm deformation has been studied in numerous papers [20, 46-47]. It was shown that the kinetics of continuous dynamic recrystallization could be adequately described by the modified Johnson-Mehl-Avrami-Kolmogorov equation. This approach used the ultra-fine grain fraction for the quantitative assessment of the continuous dynamic recrystallization progress. On the other hand, the evolution of triple junctions in dynamic recrystallized microstructures has not been detailed, although it can also be used to characterize the grain refinement kinetics during cold-to-warm deformation. Thus, the aims of the present work are to study the effect of ECAP on the microstructure evolution and the grain refinement kinetics in a Cu-Cr-Zr alloy using the triple junction distribution analysis.

2. Materials and Methods

A Cu-Cr-Zr alloy (Cu–0.1 Cr–0.07 Zr, all in wt.%) subjected to a solution treatment at 1093 K for 1 h followed by water quenching was used as the starting material. The initial grain size was about 120 μm. ECAP was used as a method of severe plastic deformation. The billets of 14 mm × 14 mm × 90 mm were processed by ECAP via route B_C (90° anticlockwise rotation of the samples after each ECAP pass) at a strain rate of 1 s^{-1}. The true strain attained at each pass was 1. ECAP was executed to different total strains up to 12. The fine microstructure of ECAP samples was examined by a Quanta 250 Nova scanning electron microscope equipped with an electron backscattering diffraction (EBSD) analyzer using an orientation imaging microscopy (OIM) software. The microstructural investigations were carried out on the Y plane, i.e. flow plane along the side face at the point of exit from the die [27]. The specimens for the EBSD analysis were electro-chemically polished at 238 K using an electrolyte of HNO_3:CH_3OH=1:3. The step size for the EBSD scan was t = 420 nm for the specimen deformed to a total strain of ε = 1, t = 200 nm for the specimen deformed to ε = 2 and t = 50 nm for specimens deformed to total strains of 4 to 12. The OIM images were processed by the clean-up procedures, setting a minimal confidence index of 0.1. The mean grain size (D) was measured by the linear intercept method on the OIM images as an interval between high-angle boundaries. A critical misorientation angle between low-angle and high-angle boundaries was 15°. The dislocation densities were estimated using the kernel average misorientations over a distance of

Preprints (www.preprints.org) | NOT PEER-REVIEWED | Posted: 1 December 2017 doi:10.20944/preprints201712.0009.v1

Peer-reviewed version available at Materials 2017, 10, 1394; doi:10.3390/ma10121394

400 nm [21]. The fraction of high-angle boundaries (F_{HAB}) and fraction of ultra-fine grains (F_{UFG}), i.e., those with D < 2 μm, were evaluated using the OIM software (EDAX TSL, version 5.2). The triple junctions fraction was estimated counting more than 300 junctions for each state. The tensile tests were executed at ambient temperature using an Instron 5882 tensile machine with an initial strain rate of 2×10^{-3} s^{-1}.

3. Results

3.1 Microstructural evolution

After solution treatment, the initial microstructure of the Cu-0.1Cr-0.06Zr alloy included coarse grains with the size of about 120 μm. Typical deformation microstructures developed in the Cu-0.1Cr-0.06Zr alloy subjected to ECAP deformation to various strain levels are shown in Fig. 1. ECAP to a relativity small strain of about 1 is accompanied by the elongation of initial coarse grains along the metal flow direction. The deformation microbands bounded by high-angle boundaries and many strain-induced subboundaries with low-angle misorientations (θ < 15°) are formed within the initial grains. Further deformation results in the deformation microbands development. The deformation microbands separate the initial grains into fragments with a size less than 10 μm. Increasing the transverse boundaries misorientation angle within the deformation microbands with straining results in the ultra-fine grain formation. An increase in the deformation microband number promotes the development of new ultra-fine grains and leads to the partially recrystallized microstructure. After a total strain of 8 many subboundaries transform into high-angle boundaries, so uniform equiaxed grains with the mean grains size below 1 μm are developed. Further deformation does not lead to any qualitative changes of the deformation microstructures.

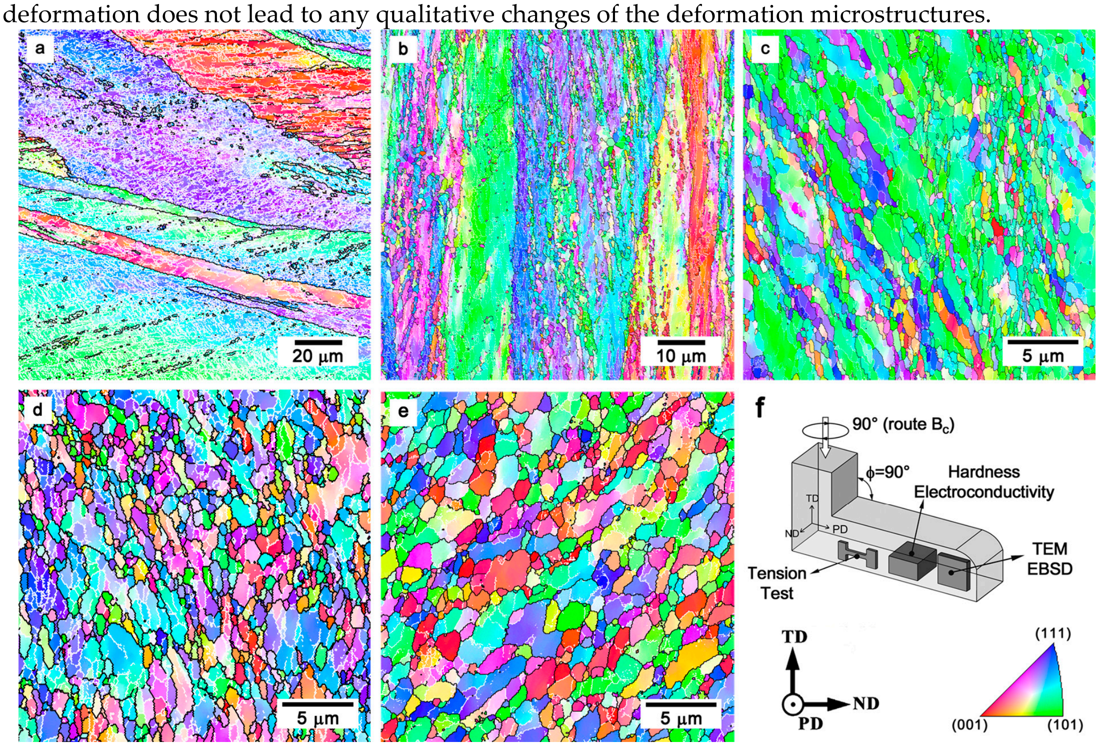

Figure 1. Typical deformation microstructures developed in a Cu-0.1Cr-0.06Zr alloy subjected to ECAP at a temperature of 673 K to total strains of 1 (a); 2 (b), 4 (c), 8 (d) and 12 (e). The inverse pole figures are shown for the pressing direction (PD in f). The white and black lines indicate the low-angle (θ<15°) and high-angle (θ≥15°) boundaries, respectively.

As can be seen in Figure 2, the grain size distribution is characterized by a low fraction of the ultra-fine grained structure near 0.05 at a relatively small strain of ε~2. The strain increasing promotes the ultra-fine grain formation and a substantial increase in the ultra-fine grain area fraction after 4 ECAP passes. The fraction of large grains decreases, while that of fine grains increases upon further processing. Thus, after total strain of 8 the ultra-fine grain fraction is above 0.5. Finally, a rather large peak stands out for small grain sizes.

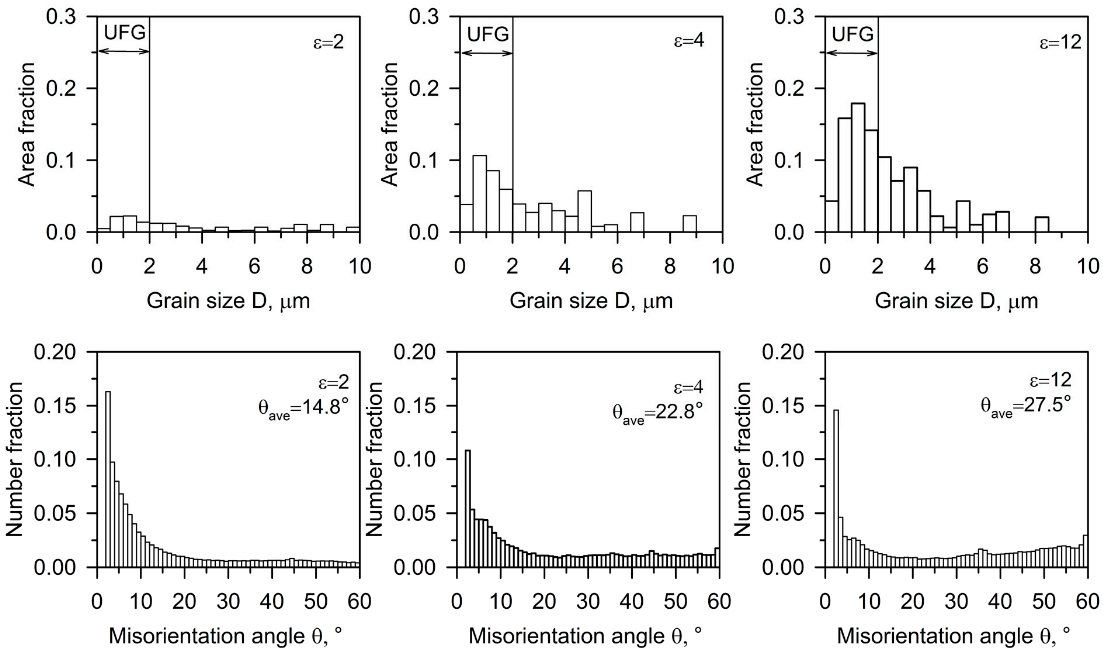

Figure 2. Grain size and boundary misorientation distributions for a Cu–0.1Cr–0.06Zr alloy processed by ECAP at 673 K to total strains (ε) of 2 to 12.

The (sub)grain misorientations developed in the Cu-Cr-Zr alloy during the severe plastic deformation by ECAP are presented in Fig. 2. The large fraction of low-angle boundaries is observed after the second ECAP pass. Then, the maximum against low-angle misorientations gradually decreases, and the fraction of high-angle misorientations increases with straining. Such flat-type misorientation distribution is often observed in various metal and alloys during severe plastic deformation accompanied by continuous dynamic recrystallization irrespective of the processing method [19-21, 37-39].

The changes in the grain size (D), the dislocation density (ρ), the high-angle boundaries fraction (F_{HAB}) and the ultra-fine grain fraction (F_{UFG}) during ECAP are shown in Figure 3. ECAP produces substantial grain refinement in the range of strains from 1 to 4. After the first ECAP pass, the mean grain size drastically reduces to 8.6 μm. Further deformation promotes grain refinement and the mean grain size after 4 ECAP passes is less than 1 μm. Then, the rate of grain refinement slows down, after total strain of ε = 12 the mean grain size attains 0.5 μm. The ECAP processing is accompanied by a significant increase in the dislocation densities from 5×10^{12} m^{-2} in the initial state to about 9×10^{14} m^{-2} after straining to 8. It is seen in Fig. 3 that the dislocation density change during ECAP clearly correlates with the grain size reduction.

The kinetics of the dynamic recrystallization during large plastic deformation can be estimated using the high-angle boundary fractions (F_{HAB}) and ultra-fine grain fractions (F_{UFG}). An increase of the ultra-fine grain fraction has an incubation period corresponding to relativity low strains of 0–2. Then, the ultra-fine grain fraction significantly increases and after a total strain of 12 attains 0.5. In contrast, the high-angle boundaries fraction gradually increases from 0.1 to its apparent saturation of about 0.7 with increasing the total strain from 1 to 12. This behavior of ultra-fine grain and high-angle boundary evolution is associated with the microbands, which are bounded by high-angle boundaries, but do not involve ultra-fine grains at relatively small strains.

Peer-reviewed version available at *Materials* **2017**, *10*, 1394; doi:10.3390/ma10121394

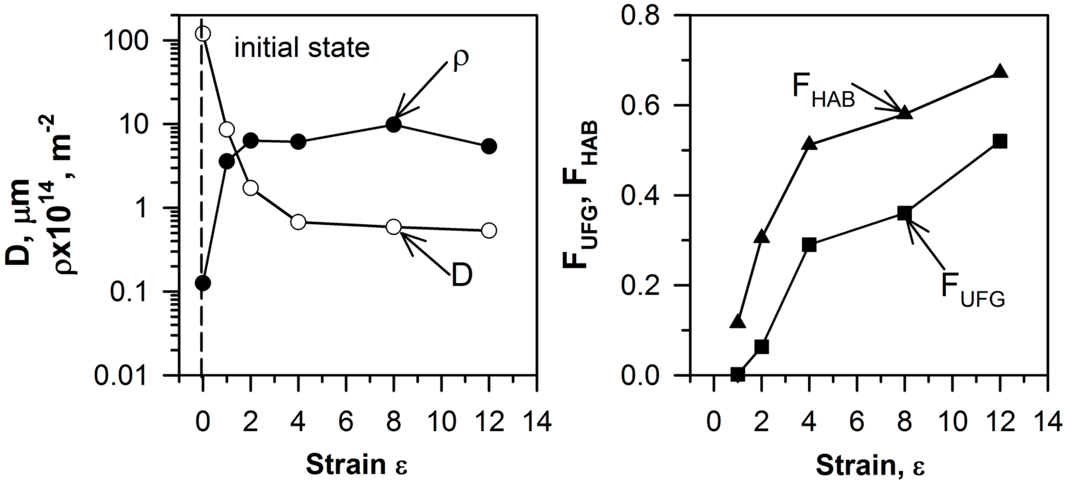

Figure 3. The strain (ε) effect on the mean grain size (D), the dislocation density (ρ), the fraction of high-angle boundaries (F_{HAB}), and the fraction of ultra-fine grain (F_{UFG}) in a Cu-0.1Cr-0.06Zr alloy subjected to ECAP at 673 K.

3.2. Tension behavior

The solution treated samples of the Cu-0.1Cr-0.06Zr alloy are characterized by the small yield strength ($\sigma_{0.2}$) of 60 MPa and the ultimate tension stress (UTS) of 185 MPa comparable to pure copper [16]. The hardening stage is large and the elongation amounts 60 % in tensile tests (Fig. 4). The strain imposed by ECAP to the copper alloy strongly influences the strength and ductility. The first pass results in significant strengthening, $\sigma_{0.2}$ and UTS increase by about 375% and 70%, respectively. Then, efficiency of deformation strengthening degrades, after the second ECAP pass additional increments in the both $\sigma_{0.2}$ and UTS are 75 MPa. Upon further straining to 4-12, the $\sigma_{0.2}$ and UTS values increase slowly, leading to gradual strengthening.

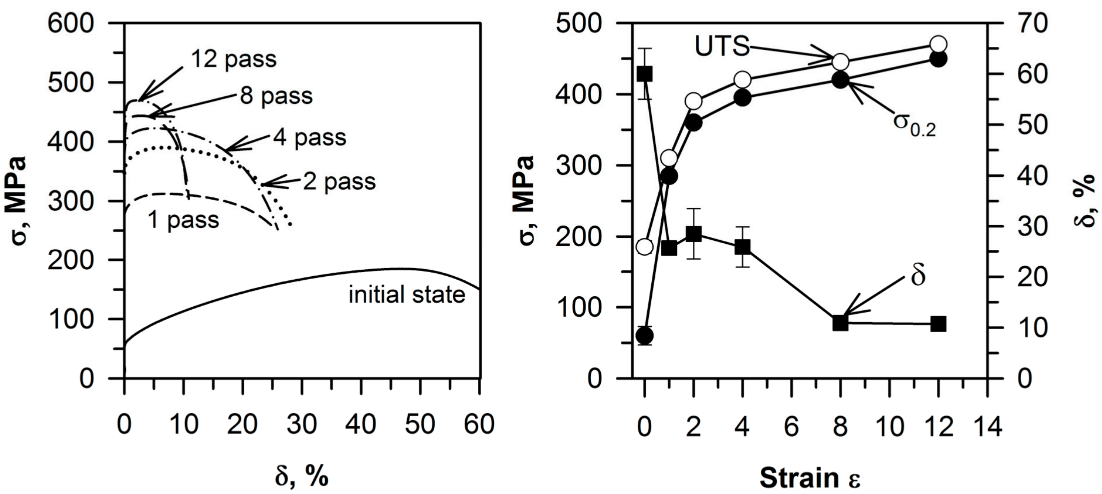

Figure 4. Stress-strain curves and the strain effect on the yield strength, ($\sigma_{0.2}$), the ultimate tensile strength (UTS) and total elongation (δ) of a Cu-0.1Cr-0.06Zr alloy subjected to ECAP at 673 K.

The maximum $\sigma_{0.2}$ and UTS are 445 MPa and 465 MPa after 12 ECAP passes, respectively. The strengthening by deformation to strains of 12 leads to a degradation in the plasticity. Total elongation decreases from 60% in the initial state to 11% after 12 passes of ECAP. The severe plastic deformation of the Cu–Cr–Zr alloy shortens the hardening stage. In contrast to the initial state, the necking in the ECAP processed samples takes place at relatively small tensile strains, leading to rapid fracture during the tensile tests. As a result, the UTS and $\sigma_{0.2}$ values are very close to each other in the Cu–0.1Cr–0.05Zr alloy subjected to the ECAP processing.

4. Discussion

The severe plastic deformation is accompanied by significant microstructure change that is associated with an increase in the dislocation density and the strain-induced (sub)boundaries. The new grains develop heterogeneously that is assisted with the formation of deformation bands. This process promotes fragmentation of the initial grains and leads to a rapid increase in the F_{HAB} fraction, while F_{UFG} does not increase remarkably at early stage of deformation (Fig. 3). The number of the deformation microbands rapidly increases during ECAP to a strain of 2. Then, the new ultra-fine grains readily develop along the microbands and the initial grain boundaries, as well as their intersections accelerating an increase in F_{UFG}. The deformation microbands and the new (sub)boundaries lead to the appearance of new triple junctions formed by low-angle and/or high-angle boundaries. The number of high-angle boundaries in the triple junctions and the distribution of the triple junction fractions are controlled by continuous dynamic recrystallization and grain refinement.

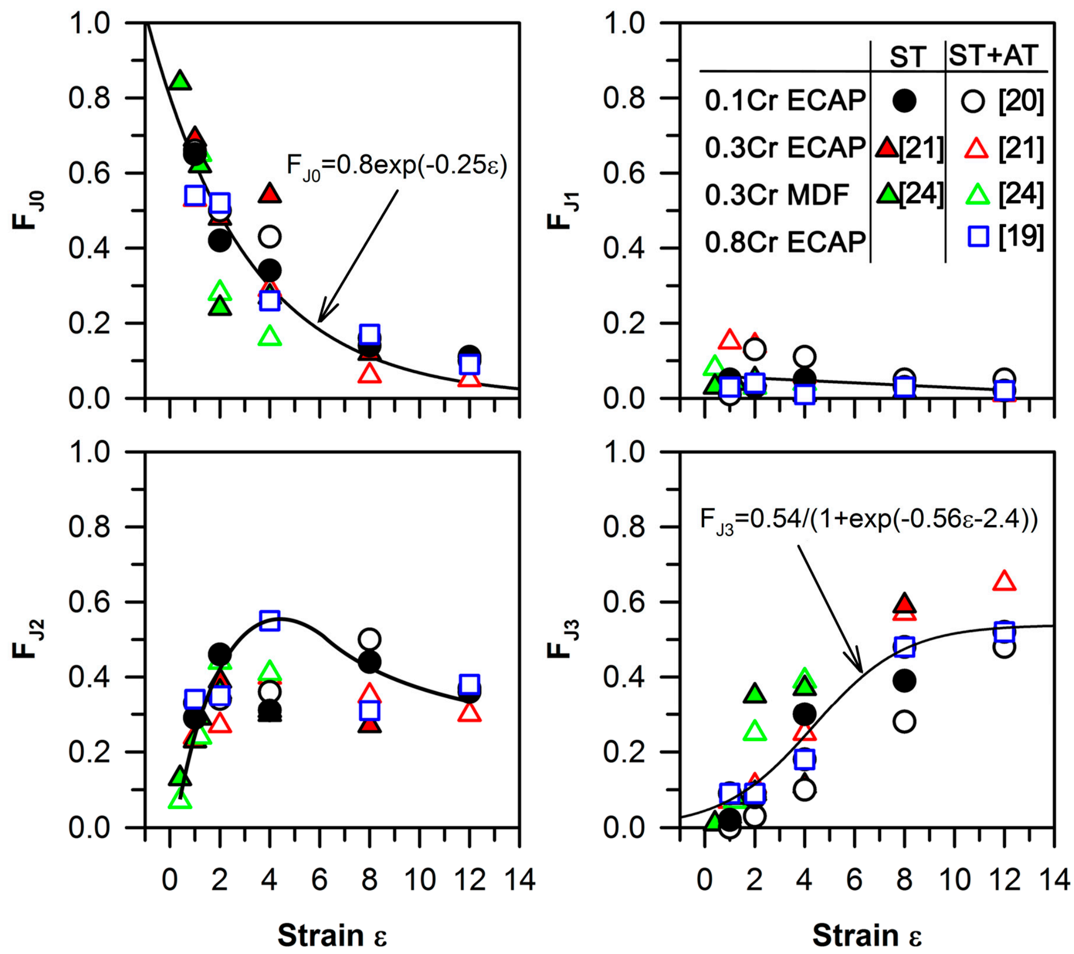

Figure 5. The strain effect on the fraction of triple junctions with 0, 1, 2 or 3 adjacent high-angle boundaries, denoted as F_{J0}, F_{J1}, F_{J2} and F_{J3}, respectively, for a Cu-0.1Cr-0.06Zr (0.1Cr), Cu-0.3Cr-0.5Zr (0.3Cr), Cu-0.8Cr-0.05Zr (0.8Cr) alloys after solution treatment (ST) or aging (AT) subjected to ECAP or multidirectional forging (MDF) at 673 K.

The effect of total strain on the fraction of triple junctions with the different contents of high-angle boundaries in the present alloy and several other Cu-Cr-Zr alloys with different chromium/zirconium contents subjected to severe plastic deformations by different methods at a temperature of 627 K [19-21, 24] is represented in Fig. 5. The large fraction of J0 at the relativity small strains corresponds to the formation of many dislocation subboundaries with low-angle misorientations. Then, the fraction of J0 gradually decreases with straining as the new high-angle boundaries develop. It should be noted that the number of the J1 junctions is quite small and does not vary remarkably during the deformation irrespective of total strains. The J1 fraction is almost unchanged with straining and equals 0.1-0.15. In contrast, many triple junctions with 2 high-angle boundaries rapidly appear upon the plastic deformation to strains of 4. Therefore, the J2 fraction quickly increases in the strain range of 0 to 4 followed by a slight decrease during subsequent deformation. The fraction of J3 exhibits an accelerated increase in the range of intermediate strains of 2 to 8 and then approaches an apparent saturation of about 0.5 at large strains. The strain range of 0 to 4 is characterized by the development of the deformation microbands. The formation of such bands leads to an increase in the J2 fraction and a decrease in the J0 fraction. The change in the J0 fraction during large deformation of the Cu-Cr-Zr alloys with different Cr and Zr content as shown in Fig. 5 can be related to the strain (ε) through an exponential function:

$$F_{J0} = 0.8 \exp(-0.25\,\varepsilon).$$

The high J2 and low J0 fractions indicate the localization of deformation in the microbands. The strain dependence of J2 fraction on ECAP deformation has a peak at total strains of 4-6. Further plastic deformation is accompanied with a decrease in the fraction of low-angle boundaries, thus, the J0 fraction degrades to almost zero at sufficiently large strains. The transformation of the transverse low-angle boundaries into high-angle boundaries and the ultra-fine grained structure formation lead to an increase in the J3 fraction while the J2 fraction decreases in the range of total strains of 8-12. The strain effect on the J3 fraction in the various Cu-Cr-Zr alloys shown in Fig. 5 can be approximated by a sigmoid law as follows:

$$F_{J3}=0.54 \,/\, (1+\exp(-0.56\,\varepsilon - 2.4)).$$

The faster structural changes during multidirectional forging as compared to ECAP may be caused by a frequent rotation of the samples around three orthogonal axes with a respect of forging direction (i.e., in each pass strain of 0.4 during multidirectional forging against a pass strain of 1.0 during ECAP).

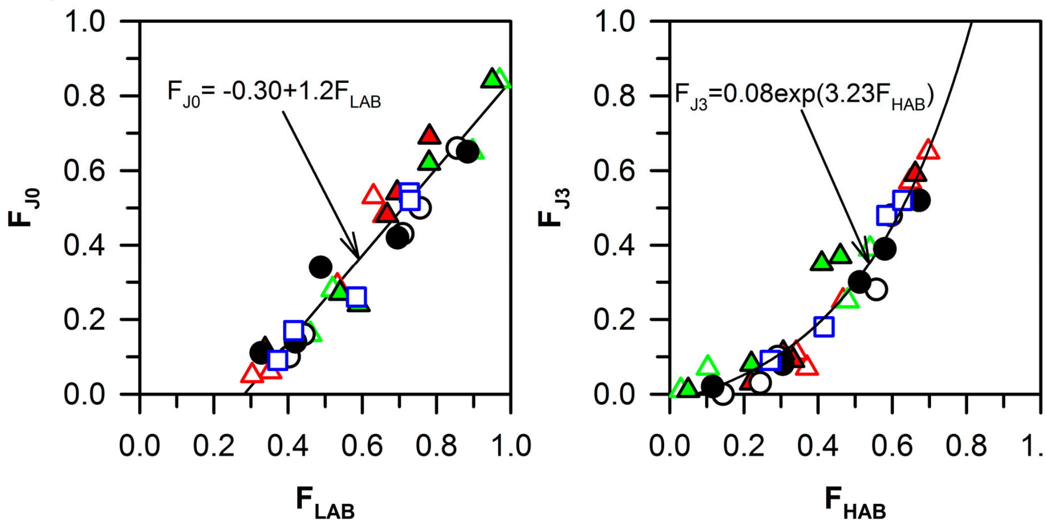

Figure 6. The relationship between the low-angle (F_{LAB}) and high-angle (F_{HAB}) boundary fractions and the fractions of triple junctions with 0 (F_{J0}) and 3 (F_{J3}) adjacent high-angle boundary in the Cu-Cr-Zr alloys after severe plastic deformation at 673 K. The type and colors of symbol have the same definitions as in Fig. 5.

Preprints (www.preprints.org) | NOT PEER-REVIEWED | Posted: 1 December 2017 doi:10.20944/preprints201712.0009.v1

Peer-reviewed version available at *Materials* **2017**, *10*, 1394; doi:10.3390/ma10121394

The J0 fraction depends on low-angle boundaries quantity and should correlate with the low-angle boundaries fraction. Figure 6 illustrates the relationship between the J0 fraction, including only low-angle boundaries, and the low-angle boundaries fraction. It can be seen that the experimental data can be expressed by a linear function as follows.

$$F_{J0} = -0.30 + 1.2\ F_{LAB}.$$

On the other hand, the high-angle boundaries fraction should correlate with the fraction of J3 triple junctions. The change in the J3 fraction with the change in the high-angle boundaries fraction in Fig. 6 can be expressed by an exponential law:

$$F_{J3} = 0.08 \exp\ (3.23\ F_{HAB}).$$

The high-angle boundaries fraction has been suggested to correlate with the ultra-fine grain fraction [19-20, 24, 38]. The relationship between F_{HAB}, F_{UFG} and F_{J3} is represented in Figure 7. The rapid growth of the high-angle boundaries fraction is associated with the appearance of deformation bands. The ultra-fine grain formation requires the high-angle misorientations for all boundaries surrounding the crystallite. Therefore, the formation of ultra-fine grains is delayed at early deformation stage until the density of high-angle boundaries attains sufficiently large value. In contrast the J3 fraction clearly correlates with the ultra-fine grain fraction and can be expressed by a linear function passing through the origin:

$$F_{J3} = 0.76\ F_{UFG}.$$

The triple junctions consisting of only high-angle boundaries and ultra-fine grained structure start to form at the same time, but the rate of ultra-fine grain formation is faster than that of increase of the J3 fraction. The lag of the J3 fraction increase is associated with a difference between the upper level of ultra-fine grain size (2 μm) and the subgrain size (0.3-0.5 μm).

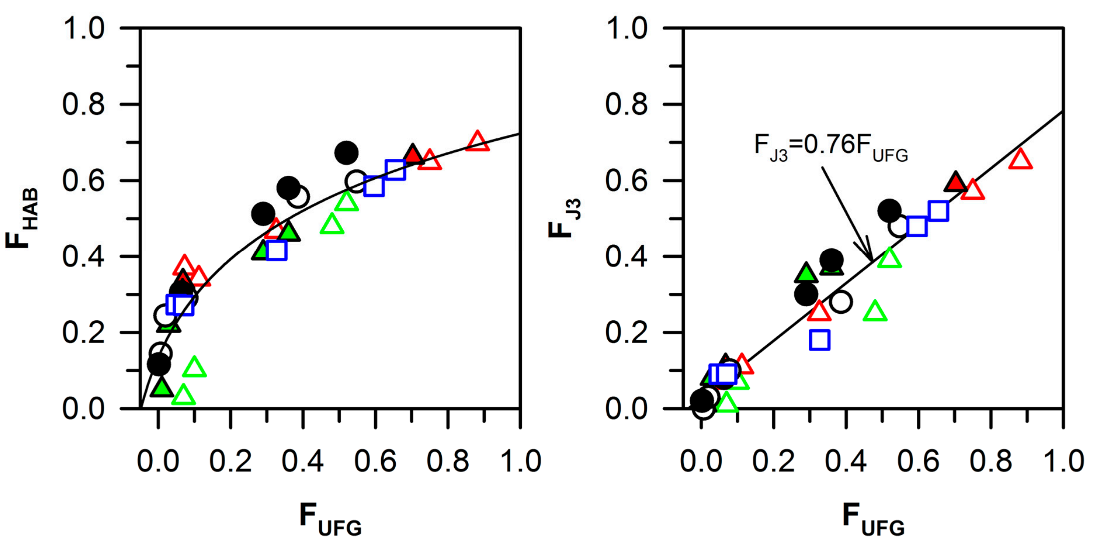

Figure 7. Relationships between the ultra-fine grain fraction (F_{UFG}), the high-angel boundary fraction (F_{HAB}) and the fraction of triple junctions of high-angle boundaries (F_{J3}) in the Cu-Cr-Zr alloys after severe plastic deformation at 673 K. The type and colors of symbol have the same definitions as in Fig. 5.

The correlation of the J3 fraction with the ultra-fine grain fraction makes it possible to use the J3 analysis to estimate the kinetics of grain refinement that can be discussed in the term of dynamic recrystallization kinetics using Eq. 1. During dynamic recrystallization, the change of the J3 fraction should correspond to the fraction of DRX grains. Therefore, the Johnson-Mehl-Avrami-Kolmogorov equation using the triple junctions approach has a similar form:

Preprints (www.preprints.org) | NOT PEER-REVIEWED | Posted: 1 December 2017 doi:10.20944/preprints201712.0009.v1

Peer-reviewed version available at Materials 2017, 10, 1394; doi:10.3390/ma10121394

$$F_{J3} = 1 - \exp(-k\varepsilon^n). \quad (2)$$

The plot of $\ln(1/(1-F_{DRX}))$ vs ε in logarithmic scale should represent a straight line. The change in the J3 fraction for the Cu-0.1 Cr-0.05 Zr and Cu-0.3 Cr -0.5Zr alloys in solution treated and aged conditions are presented in Figure 8 a and b. It is clearly seen that the J3 evolution kinetics in these two alloys is nearly the same for the solid solution conditions and can be described by the Johnson-Mehl-Avrami-Kolmogorov equation with constants of n=1.49, k=0.03. On the other hand, the aged Cu-Cr-Zr alloys with different chromium content demonstrate the different J3 fraction changing rate. The chromium increase leads to the acceleration of J3 changing kinetics, constants of n=1.16, k =0.06 are obtained for the Cu-0.3 Cr 0.5Zr alloy and those of n=1.46, k=0.03 for the Cu-0.1 Cr-0.05 Zr alloy. The promotion of the DRX kinetics has been discussed as results of particle precipitation in the starting materials [48, 49]. Therefore, the difference in the volume fraction of Cr- and Zr- particles in the Cu-Cr-Zr alloys can lead to increasing the J3 changing kinetics in the Cu-0.3Cr -0.5Zr alloy.

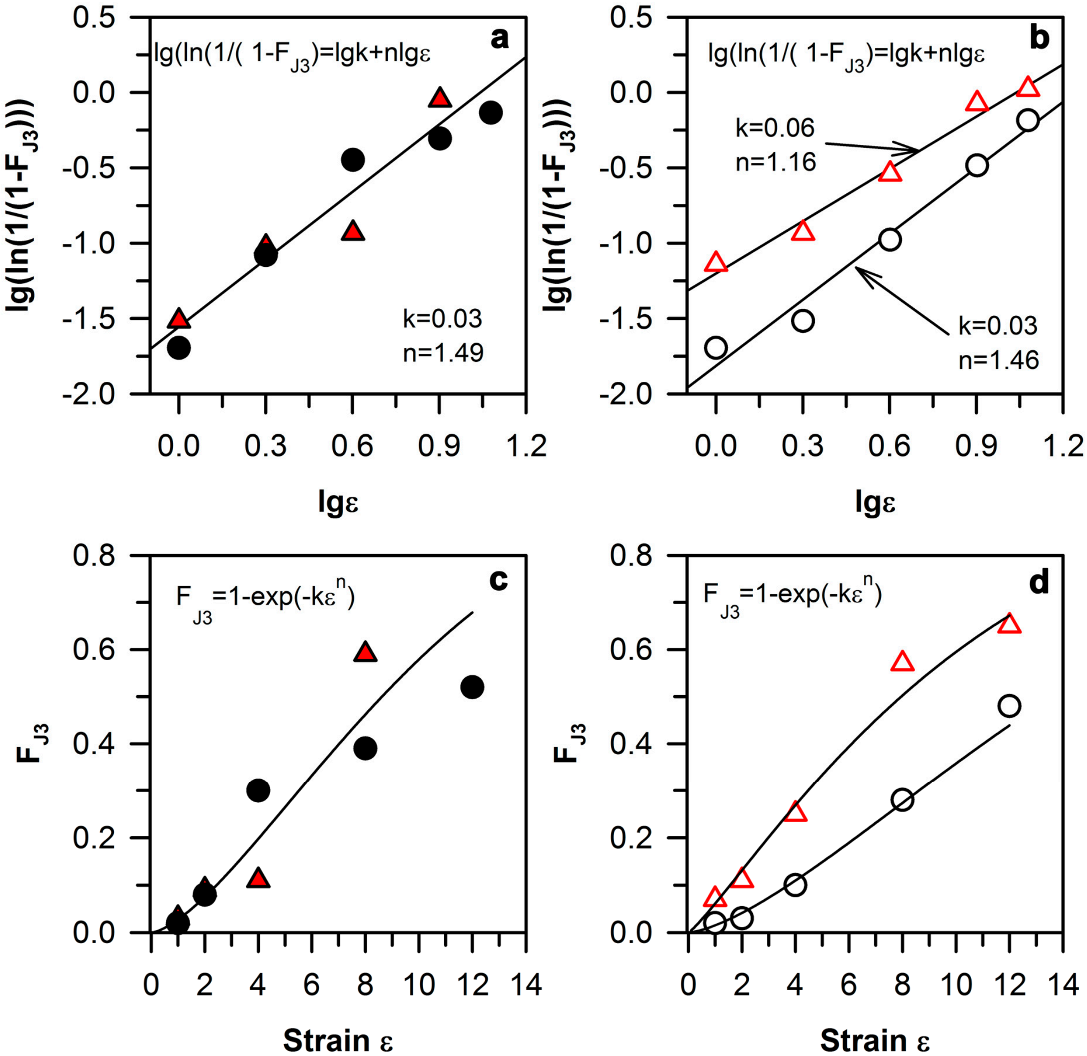

Figure 8. The strain effect on the grain refinement in a Cu-0.1Cr-0.06Zr and Cu-0.3Cr-0.5Zr alloys during ECAP at 673 K; recrystallization kinetics for solution treated (a) and aged (b) samples and the strain effect on the ultra-fine grain fraction in solution treated (c) and aged (d) samples. The type and colors of symbol have the same definitions as in Fig. 5.

Preprints (www.preprints.org) | NOT PEER-REVIEWED | Posted: 1 December 2017 doi:10.20944/preprints201712.0009.v1

Peer-reviewed version available at *Materials* **2017**, *10*, 1394; doi:10.3390/ma10121394

The obtained relationships between J0 and low-angle boundaries, J3 and high-angle boundaries/ultra-fine grains, as well as clear correlation between the qualitative microstructure evolution and the quantitative variation of the J0, J1, J2 and J3 fractions makes it possible to use the triple junction analysis as an informative source for understanding the structural changes during deformation. The presented approach using the triple junction analysis describes well the microstructural evolution during plastic deformation and allows us to study the grain refinement and dynamic recrystallization in more detail.

5. Conclusions

The grain refinement, microstructure evolution and kinetic of dynamic recrystallization in the Cu-0.1Cr-0.06Zr alloy subjected to ECAP processing at 673 K were studied using the boundary triple junction analysis. The main results can be summarized as follows:

1. The ECAP processing was accompanied by a significant decrease in the grain size from 120 μm in the initial condition to 0.5 μm after a total strain of 12. The grain size rapidly decreased during 1-4 ECAP passes and then remained almost unchanged during further ECAP.
2. The formation of the ultra-fine grained structure resulted from the deformation band evolution and an increase in misorienations of strain-induced subboundaries during ECAP-processing. An increase in total strain led to an increase in both the high-angle boundary fraction and the ultra-fine grain fraction. The grain refinement can be discussed in the terms of continuous dynamic recrystallization.
3. The ECAP-deformation was accompanied by gradual strengthening. The yield strength increased from 60 MPa in the initial state to 445 MPa after 12 ECAP passes. Correspondingly, total elongation decreased from 60% to 9%.
4. The fraction of boundary triple junctions consisting of only low-angle boundaries gradually decreased through an exponential law function of total strain during severe plastic deformation. The fraction of boundary triple junctions with one high-angle boundary and two low-angle boundaries was about 0.1-0.15 and did not change remarkably with straining. The fraction of boundary triple junctions with two high-angle boundaries and one low-angle boundary increased to a peak at strains of 4-6 followed by a little decrease at large strains. The fraction of boundary triple junctions consisting of only high-angle boundaries increased by a sigmoid law function with deformation.
5. The fractions of the low-angle boundary triple junctions and the high-angle boundary triple junctions can be related to the low-angle boundary fraction and the ultra-fine grain fraction, respectively, through linear functions. The strain dependence of the high-angle boundary triple junctions can be expressed by a modified Johnson-Mehl-Avrami-Kolmogorov equation, $F_{J3} = 1 - \exp(-k\,\varepsilon^n)$, with a strain exponent of n = 1.49 and k = 0.03.

Acknowledgments: The financial support received from the Ministry of Science and Education of Russia under the Grant No. 14.575.21.0135 (ID RFMEFI517X0135) and the technical assistance of the Joint Research Center, "Technology and Materials", Belgorod National Research University, are gratefully acknowledged.

Author Contributions: A.M. carried out severe plastic deformation and tensile tests. A.M., S.Z., A.B. and R.K. analyzed the structural changes and the dynamic recrystallization behavior. E. B. and V. B. proposed analysis of microstructure evolution in terms of the triple junctions. All authors discussed and analyzed the obtained results.

Conflicts of Interest: The authors declare no conflict of interest.

Preprints (www.preprints.org) | NOT PEER-REVIEWED | Posted: 1 December 2017 doi:10.20944/preprints201712.0009.v1

Peer-reviewed version available at *Materials* **2017**, *10*, 1394; doi:10.3390/ma10121394

References

1. Tang, N. Y., D. M. R. Taplin, and G. L. Dunlop. Precipitation and aging in high-conductivity Cu–Cr alloys with additions of zirconium and magnesium. Mater. Sci. Technol. 1985, 1.4, 270-275, DOI 10.1179/mst.1985.1.4.270.
2. Correia, J. B., Davies, H. A., Sellars, C. M. Strengthening in rapidly solidified age hardened Cu- Cr and Cu-Cr- Zr alloys, Acta Mater. 1997, 45(1), 177-190, DOI 10.1016/S1359-6454(96)00142-5.
3. Fujii, T., Nakazawa, H., Kato, M., Dahmen, U. Crystallography and morphology of nanosized Cr particles in a Cu–0.2% Cr alloy, Acta Mater. 2000, 48(5), 1033-1045, DOI 10.1016/S1359-6454(99)00411-5.
4. Batra, I.S., Dey, G.K., Kulkarni, U.D., Banerjee S., Microstructure and properties of a Cu–Cr–Zr alloy, J. Nucl. Mater. 2001, 299, 91-100, DOI 10.1016/S0022-3115(01)00691-2.
5. Chibihi, A., Sauvage, X., Blavette, D., Atomic scale investigation of Cr precipitation in copper, Acta Mater. 2012, 60, 4575-4585, DOI 10.1016/j.actamat.2012.01.038.
6. Shangina, D. V., Bochvar, N. R., Morozova, A. I., Belyakov, A. N., Kaibyshev, R. O., Dobatkin, S. V. Effect of chromium and zirconium content on structure, strength and electrical conductivity of Cu-Cr-Zr alloys after high pressure torsion, Mater. Lett. 2017, 199, 46-49, DOI 10.1016/j.matlet.2017.04.039.
7. Shangina, D., Maksimenkova, Y., Bochvar, N., Serebryany, V., Raab, G., Vinogradov, A., ... & Dobatkin, S. (2016). Influence of alloying with hafnium on the microstructure, texture, and properties of Cu–Cr alloy after equal channel angular pressing. Jour. Mater. Sci. 51(11), 5493-5501.
8. Murashkin, M. Y., Sabirov, I., Sauvage, X., & Valiev, R. Z. Nanostructured Al and Cu alloys with superior strength and electrical conductivity. J. Mater. Sci. 2016, 51(1), 33-49, DOI 10.1007/s10853-015-9354-9.
9. Zhou, H.T., Zhong, J.W., Zhou, X., Zhao, Z.K., Li, Q.B. Microstructure and properties of Cu–1.0 Cr–0.2 Zr–0.03 Fe alloy, Mater. Sci. Eng. A 2008, 498, 225-230, DOI 10.1016/j.msea.2008.07.061.
10. Lu, L., Shen, Y., Chen, X., Qian, L., Lu, K., Ultrahigh strength and high electrical conductivity in copper, Science 2004, 304, 422-426, DOI 10.1126/science.1092905.
11. Peng, L., Xie, H., Huang, G., Xu, G., Yin, X., Feng, X., & Yang, Z. The phase transformation and strengthening of a Cu-0.71 wt% Cr alloy, J. Alloys Compd. 2017, 708, 1096-1102, DOI 10.1016/j.jallcom.2017.03.069.
12. Topuz, A. I. Enabling microstructural changes of FCC/BCC alloys in 2D dislocation dynamics. Mater. Sci. Eng. A 2015, 627, 381-390, DOI 10.1016/j.msea.2015.01.016.
13. Ghosh, G., Miyake, J., Fine, M. E. The systems-based design of high-strength, high-conductivity alloys. JOM 1997, 49(3), 56-60, DOI 10.1007%2FBF02914659.
14. Li, J., Petch relation and grain boundary sources, Trans. Metall. Soc. AIME 1963, 277, 239-247.
15. Kato, M., Hall–Petch Relationship and Dislocation Model for Deformation of Ultrafine-Grained and Nanocrystalline Metals, Mater. Trans. 2014, 55, 19-24, DOI 10.2320/matertrans.MA201310.
16. Hansen, N. Boundary strengthening in undeformed and deformed polycrystals, Mater. Sci. Eng. A 2005, 409, 39–45, DOI 10.1016/j.msea.2005.04.061.
17. Borodin, E. N., Mayer, A. E. Influence of structure of grain boundaries and size distribution of grains on the yield strength at quasistatic and dynamical loading. Mater. Res. Express 2017, 4(8), 085040, DOI 10.1088/2053-1591/aa8514/.
18. Valdés León, K., Munoz-Morris, M.A., Morris, D.G. Optimisation of strength and ductility of Cu–Cr–Zr by combining severe plastic deformation and precipitation, Mater. Sci. Eng. A 2012, 536, 181–189, DOI 10.1016/j.msea.2011.12.098.
19. Mishnev, R., Shakhova, I., Belyakov, A., Kaibyshev, R. Deformation microstructures, strengthening mechanisms, and electrical conductivity in a Cu–Cr–Zr alloy, Mater. Sci. Eng. A 2015, 629, 29-40, DOI 10.1016/j.msea.2015.01.065.
20. Morozova, A., Kaibyshev, R. Grain refinement and strengthening of a Cu–0.1 Cr–0.06 Zr alloy subjected to equal channel angular pressing. Phil. Mag. 2017, 97 (24), 2053-2076, DOI 10.1080/14786435.2017.1324649.
21. Zhilyaev, A. P., Shakhova, I., Morozova, A., Belyakov, A., Kaibyshev, R. Grain refinement kinetics and strengthening mechanisms in Cu–0.3 Cr–0.5 Zr alloy subjected to intense plastic deformation, Mater. Sci. Eng. A 2016, 654, 131-142, DOI 10.1016/j.msea.2015.12.038.
22. Estrin, Y., Vinogradov, A., Extreme grain refinement by severe plastic deformation: A wealth of challenging science, Acta Mater. 2013, 61, 782–817, DOI 10.1016/j.actamat.2012.10.038.
23. Zhilyaev, A.P., Langdon, T.G., Using high-pressure torsion for metal processing: Fundamentals and applications, Prog. Mater. Sci. 2008, 53, 893–979, DOI 10.1016/j.pmatsci.2008.03.002.

24. Shakhova, I., Yanushkevich, Z., Fedorova, I., Belyakov, A., Kaibyshev, R. Grain refinement in a Cu–Cr–Zr alloy during multidirectional forging. Mater. Sci. Eng. A 2014, 606, 380-389, DOI 10.1016/j.msea.2014.03.116.
25. Tikhonova, M., Dolzhenko, P., Kaibyshev, R., Belyakov, A. Grain Boundary Assemblies in Dynamically-Recrystallized Austenitic Stainless Steel. Metals, 2016, 6(11), 268, DOI 10.3390/met6110268.
26. Takata, N., Lee, S. H., Tsuji, N. Ultrafine grained copper alloy sheets having both high strength and high electric conductivity. Mater. Lett. 2009, 63(21), 1757-1760, 10.1016/j.matlet.2009.05.021.
27. Valiev, R.Z., Langdon, T.G., Principles of equal-channel angular pressing as a processing tool for grain refinement, Prog. Mater. Sci. 2006, 51, 881–981, DOI 10.1016/j.pmatsci.2006.02.003.
28. Segal, V. M., Reznikov, V. I., Drobyshevskiy, A. E., Kopylov, V. I. 1. Under an ideal condition without the frictional effect. Russ. Metall.(Metally) 1981, 1, 99-105.
29. Zhemchuzhnikova, D., Lebyodkin, M., Lebedkina, T., Mogucheva, A., Yuzbekova, D., Kaibyshev, R. Peculiar Spatiotemporal Behavior of Unstable Plastic Flow in an AlMgMnScZr Alloy with Coarse and Ultrafine Grains. Metals 2017, 7(9), 325, 10.3390/met7090325.
30. Abib, K., Azzeddine, H., Tirsatine, K., Baudin, T., Helbert, A. L., Brisset, F., Bradai, D. Thermal stability of Cu-Cr-Zr alloy processed by equal-channel angular pressing. Mater. Charact. 2016, 118, 527-534, DOI 10.1016/j.matchar.2016.07.006.
31. Dalla Torre, F.H., Pereloma, E.V., Davies, C.H.J. Strain hardening behaviour and deformation kinetics of Cu deformed by equal channel angular extrusion from 1 to 16 passes, Acta Mater. 2006, 54, 1135–1146, DOI 10.1016/j.actamat.2005.10.041.
32. Edalati, K., Imamura, K., Kiss, T., Horita, Z. Equal-channel angular pressing and high-pressure torsion of pure copper: evolution of electrical conductivity and hardness with strain. Mater. Trans. 2012, 53(1), 123-127, DOI 10.2320/matertrans.MD201109.
33. Raab, G.J., Valiev, R.Z., Lowe, T.C., Zhu, Y.T., Continuous processing of ultrafine grained Al by ECAP–Conform, Mater. Sci. Eng. A 2004, 382, 30–34, DOI 10.1016/j.msea.2004.04.021.
34. Yuan, Y., Li, Z., Xiao, Z., & Zhao, Z. Investigations on Voids Formation in Cu–Mg Alloy During Continuous Extrusion. JOM, 2017, 69(9), 1696-1700, DOI 10.1007/s11837-017-2469-5.
35. Yuan, Y., Li, Z., Xiao, Z., Zhao, Z., & Yang, Z. Microstructure evolution and properties of Cu-Cr alloy during continuous extrusion process. J. Alloys Compd. 2017., 703, 454-460, DOI 10.1016/j.jallcom.2017.01.355.
36. Zhu, C., Ma, A., Jiang, J., Li, X., Song, D., Yang, D., Chen, J. Effect of ECAP combined cold working on mechanical properties and electrical conductivity of Conform-produced Cu–Mg alloys. J. Alloys Compd. (2014), 582, 135-140, DOI 10.1016/j.jallcom.2013.08.007.
37. Rollett, A., Humphreys, F. J., Rohrer, G. S., & Hatherly, M. Recrystallization and related annealing phenomena, 2th ed.; D. Sleeman, Elsevier: Kidlington, Oxford, pp. 574, ISBN 0 08 044164 5.
38. Sakai, T., Belyakov, A., Kaibyshev, R., Miura, H., Jonas, J.J., Dynamic and post-dynamic recrystallization under hot, cold and severe plastic deformation conditions, Prog. Mater. Sci. 2014, 60, 130–207, DOI 10.1016/j.pmatsci.2013.09.002.
39. Humphreys, F.J., Prangnell, P.B, Bowen, J.R., Gholinia, A., Harris, C. Developing stable fine–grain microstructures by large strain deformation, Philos. Trans. Roy. Soc. Lond. A 1999, 357, 1663-1681.
40. Gourdet, S., Montheillet, F. A model of continuous dynamic recrystallization, Acta Mater. 2003, 51, 2685–2699, DOI 10.1016/S1359-6454(03)00078-8.
41. Bratov, V., Borodin, E. N. Comparison of dislocation density based approaches for prediction of defect structure evolution in aluminium and copper processed by ECAP. Mater. Sci. Eng. A 2015, 631, 10-17, DOI 10.1016/j.msea.2015.02.019.
42. Chen, Z., Chen, Y. Nanocrystalline gradient engineering: Grain evolution and grain boundary networks. Computational Materials Science, 141, 282-292, 2018, DOI 10.1016/j.commatsci.2017.09.047.
43. Roberts, W., In: Strength of Metals and Alloys (ICSMA-7), edited by H.J. McQueen et al. Pergamon Press: Oxford, UK, 1986.
44. Derby, B. The dependence of grain size on stress during dynamic recrystallisation. Acta Metall. 1991, 39(5), 955-962, DOI 10.1016/0956-7151(91)90295-C.
45. Belyakov, A., Zherebtsov, S., Salishchev, G. Three-stage relationship between flow stress and dynamic grain size in titanium in a wide temperature interval. Mater. Sci. Eng. A 2015, 628, 104-109, DOI 10.1016/j.msea.2015.01.036.

46. Belyakov, A., Zherebtsov, S., Tikhonova, M., Salishchev, G. Kinetics of grain refinement in metallic materials during large strain deformation. Materials Physics and Mechanics 2015, 24(3), 224-231.
47. Shakhova, I., Belyakov, A., Kaibyshev, R. Kinetics of Submicrocrystalline Structure Formation in a Cu-Cr-Zr Alloy During Large Plastic Deformation. Mater. Sci. Forum 2017, 879, 1749-1754, DOI 10.4028/www.scientific.net/MSF.879.1749.
48. Jazaeri, H., Humphreys, F. J. (2001). The Recrystallization of a highly deformed Al-Fe-Mn alloy. In: Proc. 1 st Int. Conf. on Recrystallization and Grain Growth, 27-31 Aug 2001, Aachen, Germany.
49. Gazizov, M., Malopheyev, S., Kaibyshev, R. The effect of second-phase particles on grain refinement during equal-channel angular pressing in an Al–Cu–Mg–Ag alloy. J. Mater. Sci. 2015, 50(2), 990-1005, DOI 10.1007/s10853-014-8659-4.